Article
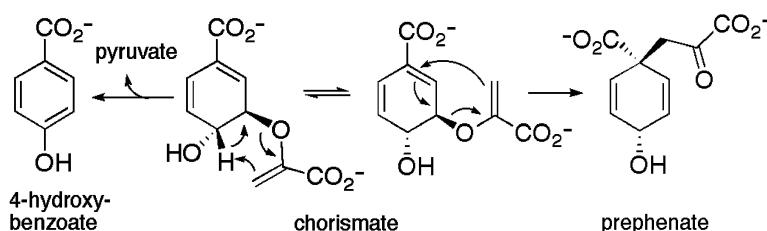
Isotope Effects on the Enzymatic and Nonenzymatic Reactions of Chorismate

S. Kirk Wright, Michael S. DeClue, Ajay Mandal, Lac Lee, Olaf Wiest, W. Wallace Cleland, and Donald Hilvert

More About This Article

Additional resources and features associated with this article are available within the HTML version:

- Supporting Information
- Links to the 5 articles that cite this article, as of the time of this article download
- Access to high resolution figures
- Links to articles and content related to this article
- Copyright permission to reproduce figures and/or text from this article

View the Full Text HTML

Isotope Effects on the Enzymatic and Nonenzymatic Reactions of Chorismate

S. Kirk Wright,[†] Michael S. DeClue,[‡] Ajay Mandal,[‡] Lac Lee,[†] Olaf Wiest,[§]
W. Wallace Cleland,[*,†] and Donald Hilvert[*,‡]

*Contribution from the Institute for Enzyme Research and Department of Biochemistry,
University of Wisconsin, 1710 University Avenue, Madison, Wisconsin 53726, Laboratory of
Organic Chemistry, Swiss Federal Institute of Technology, ETH Hönggerberg, CH-8093 Zürich,
Switzerland, and Department of Chemistry and Biochemistry, University of Notre Dame,
Notre Dame, Indiana 46556-5670*

Received May 4, 2005; E-mail: hilvert@org.chem.ethz.ch

Abstract: The important biosynthetic intermediate chorismate reacts thermally by two competitive pathways, one leading to 4-hydroxybenzoate via elimination of the enolpyruvyl side chain, and the other to prephenate by a facile Claisen rearrangement. Measurements with isotopically labeled chorismate derivatives indicate that both are concerted sigmatropic processes, controlled by the orientation of the enolpyruvyl group. In the elimination reaction of [4-^{2}H]chorismate, roughly 60% of the label was found in pyruvate after 3 h at 60 °C. Moreover, a 1.846 ± 0.057 ^{2}H isotope effect for the transferred hydrogen atom and a 1.0374 ± 0.0005 ^{18}O isotope effect for the ether oxygen show that the transition state for this process is highly asymmetric, with hydrogen atom transfer from C4 to C9 significantly less advanced than C−O bond cleavage. In the competing Claisen rearrangement, a very large ^{18}O isotope effect at the bond-breaking position (1.0482 ± 0.0005) and a smaller ^{13}C isotope effect at the bond-making position (1.0118 ± 0.0004) were determined. Isotope effects of similar magnitude characterized the transformations catalyzed by evolutionarily unrelated chorismate mutases from *Escherichia coli* and *Bacillus subtilis*. The enzymatic reactions, like their solution counterpart, are thus concerted [3,3]-sigmatropic processes in which C−C bond formation lags behind C−O bond cleavage. However, as substantially larger ^{18}O and smaller ^{13}C isotope effects were observed for a mutant enzyme in which chemistry is fully rate determining, the ionic active site may favor a somewhat more polarized transition state than that seen in solution.

The unimolecular rearrangement of chorismate (**1**) to prephenate (**2**) is a key step in the biosynthesis of the aromatic amino acids tyrosine and phenylalanine (Scheme 1). Formally, this reaction can be described as a pericyclic Claisen rearrangement, a 3,3-sigmatropic process that is rarely exploited in cellular metabolism. Secondary tritium isotope effects have suggested that the uncatalyzed reaction is concerted but asynchronous, with C−O bond cleavage preceding C−C bond formation,[1] while stereochemical studies have established a chairlike geometry for the transition state.[2] These conclusions are supported by RHF/6-31* calculations.[3]

Chorismate mutases accelerate the chorismate to prephenate rearrangement more than a million fold.[4] Crystallographic studies have shown that these enzymes fall into two structurally distinct classes.[5] The overwhelming majority of chorismate mutases belong to the AroQ family, whose prototype is the all-

Scheme 1
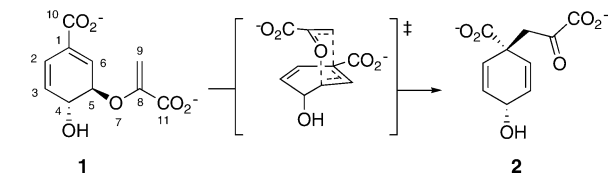
helix bundle chorismate mutase domain of the *Escherichia coli* chorismate mutase-prephenate dehydratase (EcCM).[6] The AroH class, exemplified by the monofunctional chorismate mutase from *Bacillus subtilis* (BsCM), has a trimeric pseudo α/β-barrel topology with three active sites at the subunit interfaces.[7,8] Despite their different scaffolds, the enzymes have similarly functionalized active sites, activities, and inhibition profiles.[5]

The origins of the catalytic rate enhancement achieved by chorismate mutases have been elusive. The enzymatic reactions, like their uncatalyzed counterpart, proceed via a chairlike transition state.[2] However, efforts to better define the structure

† University of Wisconsin.
‡ Swiss Federal Institute of Technology.
§ University of Notre Dame.

(1) Addadi, L.; Jaffe, E. K.; Knowles, J. R. *Biochemistry* **1983**, *22*, 4494−4501.
(2) Sogo, S. G.; Widlanski, T. S.; Hoare, J. H.; Grimshaw, C. E.; Berchtold, G. A.; Knowles, J. R. *J. Am. Chem. Soc.* **1984**, *106*, 2701−2703.
(3) (a) Wiest, O.; Houk, K. N. *J. Am. Chem. Soc.* **1995**, *117*, 11628−11639. (b) Wiest, O.; Houk, K. N. *J. Org. Chem.* **1994**, *59*, 7582−7584.
(4) Andrews, P. R.; Smith, G. D.; Young, I. G. *Biochemistry* **1973**, *12*, 3492−3498.

(5) Lee, A. Y.; Stewart, J. D.; Clardy, J.; Ganem, B. *Chem. Biol.* **1995**, *2*, 195−203.
(6) Lee, A. Y.; Karplus, P. A.; Ganem, B.; Clardy, J. *J. Am. Chem. Soc.* **1995**, *117*, 3627−3628.
(7) Chook, Y. M.; Gray, J. V.; Ke, H. M.; Lipscomb, W. N. *J. Mol. Biol.* **1994**, *240*, 476−500.
(8) Chook, Y. M.; Ke, H. M.; Lipscomb, W. N. *Proc. Natl. Acad. Sci. U.S.A.* **1993**, *90*, 8600−8603.

of this species at the active site of an AroQ enzyme, the bifunctional chorismate mutase-prephenate dehydrogenase from *E. coli*, were thwarted by suppression of the secondary tritium isotope effect, most likely due to a large forward commitment.[1] More recently, heavy atom isotope effects were determined for the BsCM-catalyzed reaction.[9] The large [18]O isotope effect at O7 (ca. 5%), the bond-breaking position, and the small, normal isotope effect at C1 (ca. 0.6%), the site of bond-making, suggested that chemistry is significantly rate determining for the AroH enzyme and that the enzymatic reaction also proceeds through a concerted but asymmetric transition state.

In the present study, we have extended our work on BsCM by determining the heavy atom isotope effect at C9 in the vinyl side chain of chorismate, providing additional information about the bond-making process. We also report heavy atom isotope effects at C1 and O7 for the EcCM-catalyzed reaction and for the uncatalyzed rearrangement of chorismate. Our results indicate that both enzyme-catalyzed reactions, as well as the spontaneous thermal reaction, proceed concertedly through similar asynchronous pericyclic transition states. Furthermore, analysis of the nonenzymatic conversion of chorismate to 4-hydroxybenzoate shows that this side reaction, which competes with the Claisen rearrangement, also proceeds via a pericyclic transition state.

Materials and Methods

General Methods and Materials. All reactions were carried out in flame-dried glassware. THF and Et_2O were dried by distillation from sodium benzophenone ketyl. CH_2Cl_2 was dried by distillation from CaH_2. All other chemicals and solvents were reagent grade and used as received. Chromatographic purifications were performed with Kieselgel 60, 230−400 mesh silica gel (Fluka). Eluent mixtures are reported as v:v percentages of the minor constituent in the major constituent. Methyl [7-^{12}C]shikimate,[10] ethyl [7-^{13}C]shikimate,[10] and potassium [3-^{13}C]phosphoenolpyruvate[11] were prepared by published methods. Unlabeled chorismic acid was isolated from *Escherichia coli* strain KA12 and purified by reverse phase chromatography.[12] Mixtures of [10-^{12}C]chorismic acid and [7-^{18}O,10-^{13}C]chorismic acid (ca. 99:1) and [10-^{12}C]chorismic acid and [1,10-^{13}C]chorismic acid (ca. 99:1) were prepared chemoenzymatically as previously described.[10] Wild-type BsCM,[13] C75S BsCM,[13] and EcCM[14] were produced and purified as reported.

[10-^{12}C]Chorismic Acid (1a). NaOH (1 M, 0.88 mL, 0.88 mmol) was added to a solution of methyl [7-^{12}C]shikimate[10] (165 mg, 0.88 mmol) in a 1:1 mixture of THF and H_2O (12 mL). The mixture was stirred at 23 °C for 8 h. After the removal of THF by distillation in vacuo, the aqueous mixture was lyophilized. The monosodium salt of ATP (0.68 g, 1.2 mmol) was dissolved in Tris-HCl (24.0 mL, 50 mM) while maintaining the pH of the solution between 6.5 and 9.0. To this solution were added FMN (50 mg, 0.09 mmol), the unlabeled monopotassium salt of phosphoenolpyruvate (0.57 g, 2.43 mmol), a solution of KCl (1.0 M aqueous, 2.0 mL), a solution of $MgSO_4$ (1.0 M aqueous, 0.2 mL), and a solution of the sodium shikimate in Tris-HCl (4.4 mL, 50 mM, pH 8.2). KA12/pKAD50 extract[15] (30 mL, corre-

sponding to the lysate of ca. 40 mg/mL) was added, and the pH of the resulting mixture was adjusted to 8.1 using NaOH (1 N). Finally, sodium dithionite (85 mg, 0.48 mmol) was added. The resulting solution was sealed and gently stirred at 23 °C for 1 h. The reaction mixture was then filtered through an Amicon 10K cutoff ultrafiltration membrane at 4 °C. When nearly dry, the membrane was washed with Tris-HCl (25 mL, 50 mM, pH 8.2). The combined filtrate was acidified to pH 1.5 and extracted with EtOAc (6 × 20 mL). The combined extracts were dried over Na_2SO_4 and carefully concentrated in vacuo (while the bath for the rotary evaporator was maintained at ca. 20 °C). The residue was dissolved in a 1:1 mixture of H_2O and MeOH and filtered through a pad of charcoal. The filtrate was lyophilized to provide crude labeled chorismic acid (80.0 mg, 40%). The residue was further purified by C-18 reverse phase silica gel chromatography (10 mM, ammonium acetate buffer). R_f (1 M, ammonium acetate buffer) 0.89. ^{1}H NMR (300 MHz, D_2O): δ 4.64 (d, J = 2.0 Hz, 1H), 4.84 (m, 1H), 4.97 (dd, J = 10.0, 2.0 Hz, 1H), 5.26 (d, J = 2.0 Hz, 1H), 6.02 (dd, J = 10, 2.0 Hz, 1H), 6.38 (dt, J = 8.0, 2.0 Hz, 1H), 6.65 (m, 1H). MS (ESI), m/z 451 (2M − H^{+}), 225 (M − H^{+}), 207 (M − H_3O^+).

[9-^{13}C,10-^{13}C]Chorismic Acid (1d). This compound was prepared chemoenzymatically from ethyl [7-^{13}C]shikimate[10] (25 mg, 0.12 mmol) and [3-^{13}C]phosphoenolpyruvate[11] (58.5 mg, 0.26 mmol), as described for [10-^{12}C]chorismic acid **1a** (8.2 mg, 30%). ^{1}H NMR (300 MHz, D_2O): δ 4.53 (m, 1H), 5.05 (dd, J = 12.6, 1.6 Hz, 1H), 5.17 (m, 1H), 5.71 (m, 1H), 6.05 (m, 1H), 6.35 (m, 1H), 6.86 (m, 1H). MS (ESI), m/z 227 (M − H^{+}), 209 (M − H_3O^+). [10-^{12}C]Chorismic acid and [7-^{18}O,10-^{13}C]chorismic acid were mixed in ca. 99:1 ratio. To ensure decomposition of all contaminating prephenate prior to determination of the isotope effect, the mixture was treated with 300 μL of 5 N HCl. After 1 h on ice, the chorismate acid solution was brought to pH to 6.5 by addition of KOH and sparged with moist CO_2-free nitrogen gas.

3-((3aS,5R,6R,6aS)-6-Benzyloxy-2,2-dimethyl-tetrahydro-furo-[2,3-d][1,3]dioxol-5-yl)-2-(diethoxy-phosphoryl)-propionic Acid Methyl Ester (4). Triflic anhydride (1.14 mL, 6.8 mmol) was added dropwise over 10 min to a stirred solution of 1,2-O-isopropylidene-3-O-benzyl-D-arabinofuranose (**3**)[16] (1.45 g, 5.2 mmol) in dry CH_2Cl_2 (15 mL) and pyridine (920 μL, 11.4 mmol) at −30 °C under a flow of nitrogen. After 15 min at −30 °C, the reaction was quenched by the addition of H_2O (5 mL). The resulting mixture was diluted with CH_2Cl_2 (20 mL), washed with aqueous NaH_2PO_4 (1.0 M, 5 mL), dried over $MgSO_4$, and evaporated to afford 2.0 g (93%) of the triflate as a light pink oil. This intermediate is highly reactive and should be used as quickly as possible. The crude triflate (2.0 g, 4.8 mmol) was dissolved in dry DMF (8.5 mL) and added to the ylid of methyl P,P-diethylphospho-nacetate, prepared in advance by adding methyl P,P-diethylphospho-nacetate (1.54 mL, 8.35 mmol) in dry DMF (8.5 mL) to a stirred suspension of sodium hydride (300 mg, 7.5 mmol) in dry DMF (20 mL) at 0 °C. After addition of 15-crown-5 (3 drops), the mixture was stirred overnight at room temperature to furnish a dark solution. The reaction was subsequently cooled to 0 °C, quenched with aqueous NaH_2PO_4 (1.0 M, 25 mL), and then extracted with $CHCl_3$ (3 × 40 mL). The combined $CHCl_3$ layers were washed with H_2O (15 mL), dried over $MgSO_4$, and evaporated to yield a red oil. Purification by flash chromatography with silica absorbent (EtOAc/hexanes, 1:1) gave 1.65 g (73%) of **4** as a mixture of diastereomers. ^{1}H NMR (300 MHz, $CDCl_3$): δ 1.28−1.37 (m, 18H), 1.51 (s, 3H), 1.55 (s, 3H), 2.15−2.30 (m, 2H), 2.35−2.55 (m, 2H), 3.04−3.20 (m, 1H), 3.34−3.50 (m, 1H), 3.68−3.86 (m, 8H), 4.06−4.22 (m, 10 H), 4.54−4.66 (m, 6H), 5.84 (d, J = 3.9 Hz, 1H), 5.89 (d, J = 3.6 Hz, 1H), 7.28−7.40 (m, 10H). HRMS-MALDI[+] [M + Na][+]: calcd ($C_{22}H_{33}NaO_9P$) 495.1760; found 495.1755.

2-(Diethoxy-phosphoryl)-3-((3aS,5R,6R,6aS)-6-hydroxy-2,2-di-methyl-tetrahydro-furo[2,3-d][1,3]dioxol-5-yl)-propionic Acid Methyl Ester (5). Compound **4** (1.65 g, 3.5 mmol) was dissolved in 40 mL of methanol and stirred with H_2O (2.0 mL), ammonium formate (1.0

(9) Gustin, D. J.; Mattei, P.; Kast, P.; Wiest, O.; Lee, L.; Cleland, W. W.; Hilvert, D. *J. Am. Chem. Soc.* **1999**, *121*, 1756−1757.
(10) Gustin, D. J.; Hilvert, D. *J. Org. Chem.* **1999**, *64*, 4935−4938.
(11) Hirschbein, B. L.; Mazenod, F. P.; Whitesides, G. M. *J. Org. Chem.* **1982**, *47*, 3765−3766.
(12) Grisostomi, C.; Kast, P.; Pulido, R.; Huynh, J.; Hilvert, D. *Bioorg. Chem.* **1997**, *25*, 297−305.
(13) Mattei, P.; Kast, P.; Hilvert, D. *Eur. J. Biochem.* **1999**, *261*, 25−32.
(14) MacBeath, G.; Kast, P.; Hilvert, D. *Biochemistry* **1998**, *37*, 10062−10073.
(15) Kast, P.; AsifUllah, M.; Hilvert, D. *Tetrahedron Lett.* **1996**, *37*, 2691−2694. Dell, K. A.; Frost, J. W. *J. Am. Chem. Soc.* **1993**, *115*, 11581−11589.

(16) Moore, B. S.; Cho, H. J.; Casati, R.; Kennedy, E.; Reynolds, K. A.; Mocek, U.; Beale, J. M.; Floss, H. G. *J. Am. Chem. Soc.* **1993**, *115*, 5254−5266.

g, 15.8 mmol), and 10% Pd/C (1.13 g) at 50 °C for 2 h. After cooling to room temperature and filtering off the Pd/C, the solution was diluted with H_2O (10 mL) and concentrated to ca. 10 mL under reduced pressure. Extraction with $CHCl_3$ (3 × 40 mL), followed by drying over $MgSO_4$ and evaporation of the solvent, afforded 1.26 g (94%) of **5** as a mixture of diastereomers as a clear oil. This material was used in the next step without further purification. ^1H NMR (300 MHz, $CDCl_3$): δ 1.27−1.36 (m, 18H), 1.50 (s, 3H), 1.54 (s, 3H), 2.16−2.51 (m, 4H), 3.02−3.50 (m, 2H), 3.73 (s, 3H), 3.76 (s, 3H), 3.96−4.18 (m, 12H), 4.51 (s, 1H), 4.53 (s, 1H), 5.86 (d, J = 3.9 Hz, 1H), 5.90 (d, J = 3.6 Hz, 1H). HRMS-MALDI$^+$ [M + Na]$^+$: calcd ($C_{15}H_{27}NaO_9P$) 405.1290; found 405.1289.

2-(Diethoxy-phosphoryl)-3-((3aS,5R,6S,6aS,[6-^2H])-6-hydroxy-2,2-dimethyl-tetrahydro-furo[2,3-d][1,3]dioxol-5-yl)-propionic Acid Methyl Ester (6). Crude **5** (1.26 g, 3.3 mmol) was stirred with phosphorus pentoxide (765 mg, 2.7 mmol) in dry DMF (12.6 mL) and dry DMSO (1.2 mL) under nitrogen at 70 °C for 3.5 h. After cooling to room temperature and dilution with H_2O (40 mL), the mixture was extracted with $CHCl_3$ (3 × 50 mL). The combined $CHCl_3$ layers were washed with H_2O (15 mL), dried over $MgSO_4$, and evaporated to give 1.1 g (88%) of the crude ketone as a light yellow oil. The latter was dissolved in methanol (27.0 mL) and water (3.0 mL) and stirred for 5 min at 0 °C. Sodium borodeuteride (590 mg, 14.1 mmol) was then slowly added to the solution over a 5 min period. After being stirred at 0 °C for 1 h, the mixture was diluted with H_2O (20 mL) and extracted with $CHCl_3$ (3 × 50 mL). The combined $CHCl_3$ layers were dried over $MgSO_4$ and evaporated to yield 940 mg (85%) of **6** as a mixture of diastereomers as a clear oil. This material was used in the next step without further purification. ^1H NMR (300 MHz, $CDCl_3$): δ 1.27−1.39 (m, 18H), 1.59 (s, 3H), 1.62 (s, 3H), 2.22−2.51 (m, 4H), 3.14−3.29 (m, 1H), 3.32−3.48 (m, 1H), 3.74 (d, J = 0.6 Hz, 3H), 3.76 (d, J = 0.6 Hz, 3H), 3.92−4.08 (m, 2H), 4.10−4.22 (m, 8H), 4.60 (s, 1H), 4.61 (s, 1H), 5.69 (d, J = 4.2 Hz, 1H), 5.72 (d, J = 4.2 Hz, 1H). HRMS-MALDI$^+$ [M + Na]$^+$: calcd ($C_{15}H_{26}DNaO_9P$) 406.1352; found 406.1352.

2-(Diethoxy-phosphoryl)-3-((3aS,4R,6aS,[3a-^2H])-6-hydroxy-2,2-dimethyl-tetrahydro-furo[3,4-d][1,3]dioxol-4-yl)-propionic Acid Methyl Ester (7). Compound **6** (940 mg, 2.45 mmol) was mixed with Dowex-50WX8-200 (2.4 g, pre-washed with acetone three times and dried under vacuum for 30 min) in dry acetone (25 mL) and stirred at room temperature under nitrogen overnight. The solution was then filtered, and the resin was washed with acetone (3 × 35 mL). The combined acetone layers were evaporated to yield 823 mg (88%) of **7** as a mixture of diastereomers as a light yellow oil. This material was used in the next step without further purification. ^1H NMR (300 MHz, $CDCl_3$): δ 1.24−1.37 (m, 18H), 1.44 (s, 3H), 1.45 (s, 3H), 2.12−2.50 (m, 4H), 3.11−3.40 (m, 2H), 3.75 (s, 6H), 4.06−4.24 (m, 10H), 4.58 (s, 2H), 5.32 (s, 2H). HRMS-MALDI$^+$ [M + Na]$^+$: calcd ($C_{15}H_{26}DNaO_9P$) 406.1352; found 406.1358.

Methyl 3,4-[4-^2H](O-Isopropylidene)shikimate (8). A solution of **7** (820 mg, 2.15 mmol) in dry methanol (60 mL) was added dropwise to a precooled solution of sodium methoxide, which was prepared by adding dry methanol (60 mL) to sodium (160 mg, 7.0 mmol, washed one time with hexanes), over 30 min under a flow of nitrogen while maintaining the temperature at 0 °C. The mixture was warmed to room temperature and stirred overnight. The reaction was then quenched by addition of a saturated aqueous solution of $NaHCO_3$ (30 mL) and extracted with Et_2O (3 × 60 mL). The combined Et_2O layers were washed with H_2O (20 mL), dried over $MgSO_4$, and evaporated to provide a light yellow oil. Purification by flash chromatography with silica absorbent (EtOAc/hexanes, 3:7) yielded 132 mg (27%) of **8** as a clear oil. ^1H NMR (300 MHz, $CDCl_3$): δ 1.40 (s, 3H), 1.45 (s, 3H), 2.03 (br s, 1H), 2.25 (ddt, J = 16.5, 8.4, 1.8 Hz, 1H), 2.80 (ddt, J = 17.4, 4.8, 0.9 Hz, 1H), 3.77 (s, 3H), 3.90 (pent, J = 3.9 Hz, 1H), 4.74 (d, J = 3.3 Hz, 1H), 6.90−6.94 (m, 1H). ^{13}C NMR (75 MHz, CD_2Cl_2): δ 25.9, 28.1, 29.8, 52.3, 69.0, 72.6, 77.9 (t, J = 22.5 Hz), 109.9,

130.9, 134.2, 166.9. HRMS-ESI$^+$ [M + Na]$^+$: calcd ($C_{11}H_{15}DNaO_5$) 252.0957; found 252.0951.

Methyl [4-^2H]Shikimate (9). Compound **8** (130 mg, 0.58 mmol) was mixed with Dowex-50WX8-200 (220 mg, washed with methanol three times and dried under vacuum for 30 min) in methanol (14 mL) containing 0.7 mL of H_2O. The mixture was stirred overnight at room temperature under an atmosphere of nitrogen. The solution was then filtered, and the resin was washed with methanol (3 × 5 mL). The combined methanol layers were evaporated to afford a light yellow oil. Purification by flash chromatography with silica absorbent (MeOH/CH_2Cl_2, 1:9) yielded 81 mg (74%) of **9** as a white solid. mp 110−113 °C. ^1H NMR (300 MHz, CD_3OD): δ 2.10 (ddt, J = 17.4, 3.9, 1.5 Hz, 1H), 2.60 (ddt, J = 18.3, 4.5, 2.1 Hz, 1H), 3.64 (s, 3H), 3.89 (t, J = 5.1 Hz, 1H), 4.27 (t, J = 1.8 Hz, 1H), 4.50 (br s, 1H), 6.69 (pent, J = 1.8 Hz, 1H). ^{13}C NMR (75 MHz, CD_3OD): δ 31.5, 51.0, 67.2, 68.4, 72.2 (t, J = 22.5 Hz), 130.2, 139.2, 168.8. HRMS-ESI$^+$ [M + Na]$^+$: calcd ($C_8H_{11}DNaO_5$) 212.0644; found 212.0643.
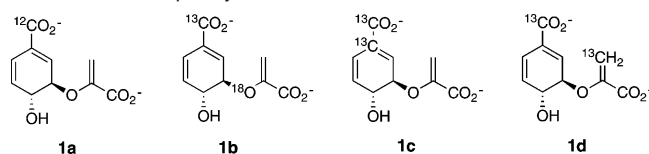
[4-^2H]Chorismate (1e). This compound was prepared chemoenzymatically from compound **9** (40 mg, 0.21 mmol) as described for [10-^{12}C]chorismic acid (**1a**).[10] It was obtained as an off-white solid (32 mg, 67%). ^1H NMR (300 MHz, D_2O, pD 6.0): δ 4.45 (d, J = 2.7 Hz, 1H), 4.78 (d, J = 2.1 Hz, 1H), 5.08 (d, J = 2.7 Hz, 1H), 5.83 (d, J = 10.8 Hz, 1H), 6.20 (dd, J = 9.9, 1.8 Hz, 1H), 6.43 (d, J = 2.1 Hz, 1H). ^2H NMR (61.4 MHz, CH_3OH): δ 4.61 (br s, 1^2H).

Kinetic Isotope Effect Measurements. All manipulations were performed on ice to suppress the nonenzymatic decomposition of chorismate. Natural abundance chorismate or mixtures of specifically labeled substrates were dissolved in 50 mM potassium phosphate buffer, pH 7.5. The chorismate concentration, determined spectroscopically at 274 nm (ϵ 2630 M^{-1} cm^{-1}), was between 1 and 2 mM for complete conversion reactions and between 4 and 6 mM for partial conversion reactions. The substrate solution (4 mL) was placed in a sidearm decarboxylation flask fitted with a stopcock adapter. The solutions were sparged with moist CO_2-free nitrogen gas. For the enzymatic reactions, the sample was warmed to 22 °C and an appropriate amount of chorismate mutase (0.25 Units) was introduced through the sidearm. Aliquots of the reaction mixture were removed, and the progress of the reaction was monitored spectroscopically at 274 nm ($\Delta\epsilon$ 2630 M^{-1} cm^{-1}). At the desired endpoint (ca. 50% or 100% conversion), the reaction was quenched by addition of 300 μL of 5 N HCl. After 45 min at room temperature, volatile products were collected under reduced pressure, using two liquid nitrogen/pentane traps (−115 °C) to remove contaminants and H_2O and a liquid nitrogen trap (−196 °C) to trap CO_2. The $^{13}CO_2/^{12}CO_2$ ratio of the sample (R_P) was then determined on a Finnigan delta E isotope ratio mass spectrometer as previously described.[9] The remaining reaction solution from partial conversion experiments was subsequently treated with KOH to bring the pH to 6.5 and sparged with moist CO_2-free nitrogen gas. Residual substrate was then completely converted to product by addition of wild-type BsCM. After 12 h at 22 °C, 5 N HCl was added and the decarboxylation reaction was allowed to proceed for 45 min. The CO_2 was distilled at reduced pressure as described above, and the $^{13}CO_2/^{12}CO_2$ ratio of the residual substrate (R_S) was determined by mass spectrometry. All reactions were performed in triplicate.

For the nonenzymatic reactions, 4 mL chorismate samples (2−4 mM) were incubated at 60 °C in the same buffer as that used in the enzyme-catalyzed reactions. The progress of the reaction was monitored by ^1H NMR and UV−vis spectroscopy. After 30 min, corresponding to conversion of ca. 50% of the starting material, the reaction was quenched with 5 N HCl, and the $^{13}CO_2/^{12}CO_2$ ratios, R_P and R_S, were determined as described above. The R_0 value for the samples, corresponding to the $^{13}CO_2/^{12}CO_2$ ratio obtained upon 100% conversion of chorismate, was obtained by adding wild-type BsCM as described above.

NMR Kinetics. The reaction of chorismate and [4-^2H]chorismate (20 mM) was monitored at 60 °C by ^1H NMR spectroscopy in deuterated phosphate buffer (200 mM, pD 7.5) containing dioxane (1.0

Scheme 2. Isotopically Labeled Chorismate Derivatives

Table 1. Kinetic Isotope Effects on the Rearrangement Catalyzed by Wild-Type BsCM, C75S BsCM, and EcCM[a]

enzyme	label		
	^{18}O-7	^{13}C-1	^{13}C-9
wt BsCM	1.045 ± 0.003[b]	1.0043 ± 0.0002[b]	1.0129 ± 0.0024
C75S BsCM	1.053 ± 0.002[b]	1.0057 ± 0.0002[b]	1.0110 ± 0.0022
EcCM[c]	1.046 ± 0.0002	1.015 ± 0.0002	n.d.
Becke3LYP 6-31+G*[d]	1.049	1.0131	1.0178

[a] In 50 mM potassium phosphate buffer, pH 7.5, and 22 °C. KIEs are corrected by division by the observed secondary kinetic isotope effect at C10, which was measured to be 1.0009 ± 0.0001 for wild-type BsCM, 1.0016 ± 0.0002 for the C75S variant, and 1.0033 ± 0.0001 for EcCM. [b] Reference 9. [c] n.d., not determined. [d] Calculated at 295.15 K.

mM) as an internal standard. The concentrations of chorismate, prephenate, phenylpyruvate, and 4-hydroxybenzoate were determined periodically by integration of representative, well-resolved peaks and comparison to the internal standard. The kinetic data were analyzed with the program DynaFit.[17] The decomposition of [4-^{2}H]chorismate in phosphate buffer (pH 6.0, 60 °C) was similarly monitored by ^{2}H NMR spectroscopy using dioxane-d_8 as the internal standard. All experiments were performed in duplicate.

Computational Studies. All calculations were performed using the G03 series of programs[18] at the B3LYP/6-31+G* level of theory. Transition structures were characterized by harmonic frequency calculations and had exactly one negative eigenvalue, corresponding to the reaction coordinate, as confirmed by intrinsic reaction coordinate (IRC) calculations. Isotope effects were calculated using QUIVER[19] and the harmonic frequencies, scaled by 0.961, at temperatures of 295.15 and 333.15 K and are corrected for tunneling with a one-dimensional tunneling approximation as proposed by Bell.[19,20] An extended, diequatorial conformation of chorismate served as the reference state for the isotope effect calculations (see Supporting Information).

Results

Labeled Chorismates. Primary heavy atom isotope effects on both the enzymatic and the nonenzymatic rearrangement of chorismate to prephenate were determined by the remote label method,[21] exploiting the C10 carboxylate of chorismate as the indicator position (Scheme 2). Prephenate decarboxylates quantitatively under acidic conditions,[22] releasing the carbon at the indicator position as CO_2. The isotopic composition of the latter was determined by isotope ratio mass spectrometry, enabling determination of isotope effects at the mechanistically interesting key positions O7, C1, and C9.

A ca. 99:1 mixture of [10-^{12}C]chorismate (**1a**) and [7-^{18}O,-10-^{13}C]chorismate (**1b**) was used to determine a primary isotope effect at the site of bond breaking, whereas ca. 99:1 mixtures of [10-^{12}C]chorismate (**1a**) and [1,10-^{13}C]chorismate (**1c**) or [9,-10-^{13}C]chorismate (**1d**) were used to determine the isotope effects at the sites of bond formation. The required chorismate derivatives were prepared chemoenzymatically. Biosynthetic transformation of mixtures of singly and doubly labeled shikimates gave the **1a**/**1b** and **1a**/**1c** mixtures, as previously described.[10] In contrast, the **1a**/**1d** mixture was prepared by mixing independently synthesized **1a** and **1d** in the desired ratio. The latter mixture was treated with acid prior to enzymatic reaction to decompose contaminating prephenate originating from either of the components, which could serve as a source of CO_2 and skew the isotopic ratios.

Enzymatic Reactions. For determination of the isotope effects on the enzymatic reaction, unlabeled chorismate contain-

ing only natural abundance ^{13}C and the **1a**/**1b**, **1a**/**1c**, and **1a**/**1d** substrate mixtures were converted enzymatically to prephenate in separate experiments. In each case, three complete conversion reactions were performed with 4−6 mM chorismate with wild-type BsCM, and three partial conversion reactions (to ca. 50%) were carried out for the wild-type enzyme, the C75S BsCM variant, and EcCM. At the desired endpoint, the reaction was quenched with 5 M HCl and volatile products were collected under reduced pressure, using two pentane/liquid N_2 traps at −115 °C to remove H_2O and other contaminants and a liquid N_2 trap at −196 °C to trap CO_2. The $^{13}CO_2/^{12}CO_2$ ratio of the sample was then determined on a Finnigan delta E isotope ratio mass spectrometer, and the heavy atom isotope effects were calculated according to eq 1:

$$KIE = \frac{\log(1 - f)}{\log[1 - f(R_P/R_0)]} \qquad (1)$$

where R_0 is the isotope ratio of the remote label in the starting material (obtained by running the reaction to completion), R_P is the isotope ratio of the remote label in the product, and f is the fractional conversion of substrate to product. The observed values for the **1a**/**1b**, **1a**/**1c**, and **1a**/**1d** mixtures were divided by the secondary kinetic isotope effect at C10, measured with unlabeled chorismate to give the desired ^{18}O and ^{13}C isotope effects.

Data for the BsCM variants are summarized in Table 1, together with theoretical isotope effects based on the transition structure for the concerted reaction obtained at the Becke3LYP/6-31+G* level of theory. As was previously reported,[9] a very large ^{18}O effect on C−O cleavage and a smaller, but still significant, ^{13}C effect at C1 are observed for the BsCM-catalyzed reactions. The 1.3% and 1.1% ^{13}C effects at C9 for the BsCM and C75S BsCM variants, respectively, confirm that C−C bond formation lags considerably behind C−O bond cleavage in the enzyme-catalyzed reaction. Data for the structurally unrelated helical bundle mutase EcCM, which are also reported in Table 1, are qualitatively similar to those obtained with BsCM. The 4.6% ^{18}O KIE at O7 and the smaller 1.5% ^{13}C KIE at C1 closely match the corresponding theoretical isotope effects.

Nonenzymatic Reactions. Chorismate decomposes with a $t_{1/2}$ of ∼30 min at 60 °C.[4] Under these conditions, elimination of the enolpyruvyl side chain to give 4-hydroxybenzoate competes with the Claisen rearrangement to prephenate, and prephenate is also further converted to phenylpyruvate, as summarized in Scheme 3.[4]

The thermal reaction can be directly monitored by ^{1}H NMR spectroscopy. A typical time course for the decomposition

(17) Kuzmic, P. *Anal. Biochem.* **1996**, *237*, 260−273.
(18) Frisch, M. J.; et al. *Gaussian 03*, revision C.01; Gaussian, Inc.: Wallingford, CT, 2004.
(19) Saunders, M.; Laidig, K. E.; Wolfsberg, M. *J. Am. Chem. Soc.* **1989**, *111*, 8989−8994.
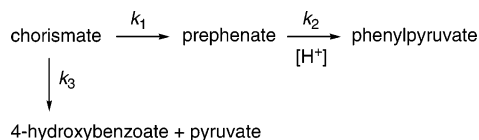(20) Bell, R. P. *The Tunnel Effect in Chemistry*; Chapman and Hall: New York, 1980; pp 60−63.
(21) O'Leary, M. H. *Methods Enzymol.* **1980**, *64*, 83−104.
(22) Zamir, L. O.; Tiberio, R.; Jensen, R. A. *Tetrahedron Lett.* **1983**, *24*, 2815−2818.
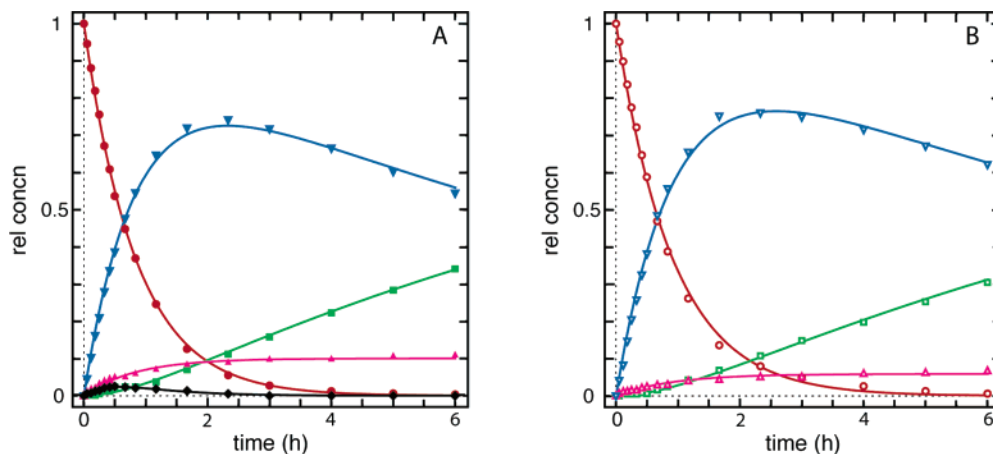
Figure 1. Kinetic analysis of the nonenzymatic decomposition of chorismate (A) and [4-²H]chorismate (B) in 200 mM phosphate buffer in D_2O at 60 °C. The reactions were monitored by ¹H NMR spectroscopy. Relative concentrations of chorismate (red ●), prephenate (blue ▼), phenylpyruvate (green ■), 4-hydroxybenzoate (magenta ▲), and pyruvate (black ◆) are plotted as a function of time. The data were analyzed with the program DynaFit.[17]

Scheme 3

Table 2. Kinetic Isotope Effects on the Thermal Reactions of Chorismate[a]

	label		
product	¹⁸O-7	¹³C-1	²H-4
prephenate	1.0482 ± 0.0005	1.0118 ± 0.0004	1.07 ± 0.04
Becke3LYP 6-31+G*[b]	1.0427	1.0119	0.87
4-hydroxybenzoate	1.0374 ± 0.0005	1.0113 ± 0.0004	1.85 ± 0.06
Becke3LYP 6-31+G*[b]	1.0465	1.0022	1.45

[a] In 100 mM potassium phosphate, pH 7.5, heated for 30 min at 60 °C. KIEs are corrected by division by the observed secondary kinetic isotope effect at C10, which was measured to be 1.0011 ± 0.002 for the formation of both prephenate and 4-hydroxybenzoic acid. The buffer concentration for the deuterium kinetic isotope effects was 200 mM. [b] Calculated at 333.15 K (see Supporting Information).

of unlabeled chorismate at 60 °C in 200 mM sodium phosphate buffer in D_2O (pD 7.5) is shown in Figure 1A. The rate constants obtained are $k_1 = (2.98 \pm 0.01) \times 10^{-4}$ s⁻¹, $k_2 = (2.59 \pm 0.05) \times 10^{-5}$ s⁻¹, and $k_3 = (3.26 \pm 0.09) \times 10^{-5}$ s⁻¹. Although a k_1/k_3 ratio of ca. 4 was previously reported based on indirect measurements of the reaction constituents,[4] we find a value of 9. Under the conditions of our experiment, the pyruvate that is produced in the elimination step also exchanges with solvent with an apparent rate constant of $k_4 = (6.8 \pm 0.6) \times 10^{-4}$ s⁻¹.

Heavy atom isotope effects on the nonenzymatic Claisen rearrangement to give prephenate, $^{18}k_1$ and $^{13}k_1$, were determined at 60 °C as described for the enzymatic reactions and calculated from the following relationship:

$$^xk_1 = \left(\frac{\log(1-f)}{\log[(1-f)(R_S/R_0)]}\right)\left(\frac{[1-(1-f)(R_S/R_0)]}{[f(R_P/R_0)]}\right) \quad (2)$$

where $^xk_1$ is the apparent isotope effect, expressed as a ratio of the rate constants for the light and heavy (x) isotopes. A derivation of eq 2 is provided in the Supporting Information. The ¹⁸O isotope effect at O7 and the ¹³C effect at C1 are in excellent agreement with the theoretical isotope effects (Table 2).

Because only small amounts of hydroxybenzoic acid are formed in the thermal reaction, it was not possible to determine the heavy atom isotope effects, $^{18}k_3$ and $^{13}k_3$, on the elimination reaction directly. However, these KIEs were estimated according to eq 3 (for a derivation, see Supporting Information):

$$^xk_3 = \frac{^xk_1}{(1 + k_1/k_3)/\alpha - (k_1/k_3)} \quad (3)$$

where $^xk_1$ is the isotope effect value obtained from eq 2, k_1 and k_3 are the rate constants for the formation of prephenate and

4-hydroxybenzoate estimated from the product distribution ratios, and $\alpha = [f(R_P/R_0)]/[1 - (1 - f)(R_S/R_0)]$. The values are summarized in Table 2.[23] The 3.74% ¹⁸O isotope effect indicates extensive C–O bond cleavage in the transition state for the elimination. The 1.13% ¹³C isotope effect at C1 reflects the decrease in bond order associated with the increase in positive charge at this site.

To gain further insight into the competing elimination reaction, [4-²H]chorismate (**1e**) was prepared chemoenzymatically according to Scheme 4. Its decomposition was monitored at 60 °C in 200 mM sodium phosphate buffer in D_2O (pD 7.5) by ¹H NMR spectroscopy as shown in Figure 1B. The rate constants obtained are $k_1 = (2.78 \pm 0.10) \times 10^{-4}$ s⁻¹, $k_2 = (2.19 \pm 0.04) \times 10^{-5}$ s⁻¹, and $k_3 = (1.77 \pm 0.03) \times 10^{-5}$ s⁻¹, affording deuterium isotope effects of 1.07 ± 0.04, 1.19 ± 0.03, and 1.85 ± 0.06 on the k_1, k_2, and k_3 steps, respectively. Based on the value of $^Dk_3$, C–H bond cleavage is not far advanced in the transition state for the elimination. The fate of the deuterium atom at C4 in this pathway was determined by ²H NMR spectroscopy at 60 °C and pH 6.0 (to minimize exchange with solvent). In addition to [4-²H]phenylpyruvate, formation of

(23) The agreement between theory and experiment is poorer for the heavy atom isotope effects on the elimination reaction than for the Claisen rearrangement, probably due to the indirect nature of the experimental determinations. The discrepancy in the case of the deuterium isotope effects can be attributed to the fact that the one-dimensional tunneling correction is insufficient. An explicit quantum mechanical treatment of the nuclear hydrogen coordinate is likely to be required, but is currently not possible for systems of this size.

Scheme 4. Synthesis of [4-^{2}H]Chorismate (**1e**)^a
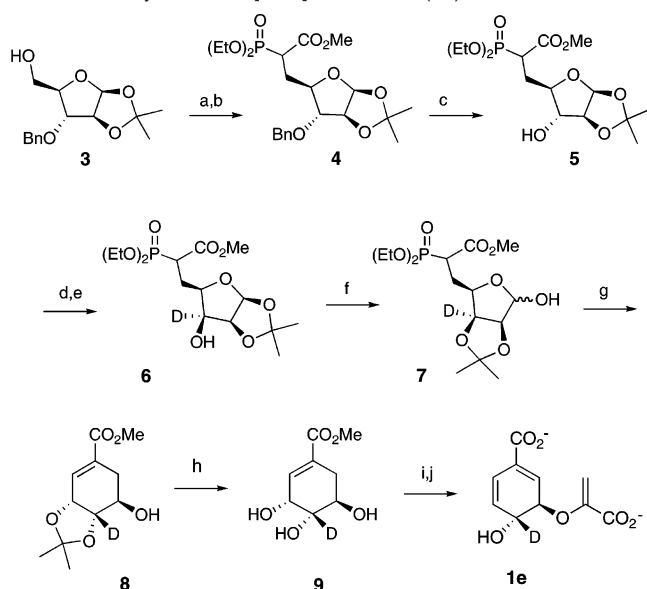
^{a} Conditions: (a) (CF$_3$SO$_2$)$_2$O, py, CH$_2$Cl$_2$, -30 °C; (b) (EtO)$_2$P(O)CH$_2$-CO$_2$Me, NaH, DMF, 83% over two steps; (c) Pd/C, MeOH, HCO$_2$NH$_4$, 50 °C, 94%; (d) P$_2$O$_5$, DMSO, DMF, 70 °C; (e) NaBD$_4$, MeOH, 0 °C, 85% over two steps; (f) Dowex-50w, acetone, 88%; (g) MeOH, Na^0, 0 °C, 27%; (h) Dowex-50w, MeOH/H$_2$O, 74%; (i) NaOH, THF, H$_2$O; (j) KA12/pKAD50, Tris-HCl, PEP, ATP, FMN, KCl, MgSO$_4$, NaS$_2$O$_4$, 67% over two steps.

[3-^{2}H]pyruvate was directly observed (Figure 2). Based on the ratio of integrated signals for pyruvate to 4-hydroxybenzoate observed by ^{1}H NMR spectroscopy after lyophilization of the sample, 62% of the pyruvate formed after 3 h contains deuterium originating from C4 of the labeled chorismate.

Discussion

Aliphatic and aromatic Claisen rearrangements have been extensively investigated by theory[24] and experiment.[25,26] High-level calculations indicate that these reactions are concerted and proceed via cyclically delocalized, chairlike transition states in which carbon–oxygen bond cleavage precedes carbon–carbon bond formation. Experimental ^{13}C and ^{2}H isotope effects have been determined by multisite NMR methods for the archetypal rearrangement of allyl vinyl ether and allyl phenyl ether, which exhibit excellent quantitative agreement with calculated isotope effects.[27] These findings provide confidence in the ability of theory to account for the multidimensional bonding changes that occur along the reaction coordinate.

For the chorismate-to-prephenate transformation, density functional theory (DFT) calculations in vacuo predict a somewhat looser aromatic transition state than the canonical aliphatic Claisen rearrangement, with bond lengths of 2.127 and 2.660 Å for the breaking C–O and forming C–C bonds, respectively (Figure 3).[9,28] In qualitative agreement with this model, secondary tritium isotope effects on the thermal reaction indicated significant cleavage of the C–O bond (ca. 40%) but little or no formation of the C–C bond.[1] The heavy atom isotope effects determined in the current study confirm and extend this picture. The very large ^{18}O effect at O7, the site of bond breaking, and the smaller, but still significant ^{13}C effect at C1, the site of bond making, are both in excellent accord with the kinetic isotope effects calculated at the Becke3LYP/6-31+G* level of theory for a pericyclic transition state (Table 1). This picture is rounded out by the observation of a small secondary ^{2}H effect for the hydrogen at C4, consistent with hyperconjugative stabilization of the developing positive charge on the ring. In this case, the agreement between theory and experiment is not as good (observed, 1.07 ± 0.04; predicted 0.87), presumably due to the fact that the dihedral angle between the hydrogen at C4 and the cyclohexadienyl ring is not predicted accurately; even relatively small changes in this angle will influence the extent of hyperconjugation, leading to significant uncertainty in the calculated isotope effect at this position. Together, the data provide strong experimental evidence that the thermal rearrangement is a concerted, albeit asynchronous, [3,3]-sigmatropic process.[29]

In principle, chorismate mutases, which accelerate this transformation more than a million-fold, could lower the energy barrier for rearrangement simply by stabilizing the pericyclic transition state observed in solution. Alternatively, the enzymes might perturb this structure or even favor alternative mechanisms, such as a two-step dissociative pathway or other routes.[30] The observation of a large ^{18}O effect at O7, and a smaller ^{13}C effect at C1, for the reaction catalyzed by the AroH mutase from *B. subtilis* had previously been used to argue that the enzymatic reaction, like its solution counterpart, is a concerted pericyclic process with some C–C bond formation accompanying C–O bond cleavage.[9] The ^{13}C isotope effect of 1.0129 ± 0.0024 at C9 of chorismate with wild-type BsCM, which was determined in the current study, strengthens this conclusion. A stepwise mechanism should be insensitive to isotopic substitution at C9, because the ion pair intermediate would be expected to partition preferentially forward to give prephenate, rather than

(24) Dewar, M. J. S.; Healy, E. F. *J. Am. Chem. Soc.* **1984**, *106*, 7127–7136. Vance, R. L.; Rondan, N. G.; Houk, K. N.; Jensen, F.; Borden, W. T.; Komornicki, A.; Wimmer, E. *J. Am. Chem. Soc.* **1988**, *110*, 2314–2315. Dewar, M. J. S.; Jie, C. *J. Am. Chem. Soc.* **1989**, *111*, 511–519. Wiest, O.; Black, K. A.; Houk, K. N. *J. Am. Chem. Soc.* **1994**, *116*, 10336–10337. Davidson, M. M.; Hillier, I. H.; Vincent, M. *Chem. Phys. Lett.* **1995**, *246*, 536–540. Yamabe, S.; Okumoto, S.; Hayashi, T. *J. Org. Chem.* **1996**, *61*, 6218–6226.
(25) Ziegler, F. E. *Chem. Rev.* **1988**, *88*, 1423–1452. Gajewski, J. J.; Conrad, N. D. *J. Am. Chem. Soc.* **1979**, *101*, 2747–2748. McMichael, K. D.; Korver, G. L. *J. Am. Chem. Soc.* **1979**, *101*, 2746–2747. Coates, R. M.; Rogers, B. D.; Hobbs, S. J.; Peck, D. R.; Curran, D. P. *J. Am. Chem. Soc.* **1987**, *109*, 1160–1170. Kupczyk-Subotkowska, L.; Saunders, W. H., Jr.; Shine, H. J. *J. Am. Chem. Soc.* **1988**, *110*, 7153–7159. Kupczyk-Subotkowska, L.; Subotkowski, W.; Saunders, W. H., Jr.; Shine, H. J. *J. Am. Chem. Soc.* **1992**, *114*, 3441–3445. Kupczyk-Subotkowska, L.; Saunders, W. H., Jr.; Shine, H. J.; Subotkowski, W. *J. Am. Chem. Soc.* **1993**, *115*, 5957–5961. Gajewski, J. J.; Brichford, N. L. *J. Am. Chem. Soc.* **1994**, *116*, 3165–3166. Gajewski, J. J. *Acc. Chem. Res.* **1997**, *30*, 219–225.
(26) Gajewski, J. J.; Jurayj, J.; Kimbrough, D. R.; Gande, M. E.; Ganem, B.; Carpenter, B. K. *J. Am. Chem. Soc.* **1987**, *109*, 1170–1186.

(27) Meyer, M. P.; DelMonte, A. J.; Singleton, D. A. *J. Am. Chem. Soc.* **1999**, *121*, 10865–10874.
(28) This structure has slightly shorter C–O and C–C bond lengths than the transition state reported previously (ref 9), but the effect on the calculated heavy atom isotope effects is small. The relative looseness of the calculated transition state probably reflects electrostatic repulsion of the negatively charged carboxylate groups in the chair geometry, as well as the known bias of the B3LYP method (ref 27).
(29) An alternative two-step mechanism involving an ion pair intermediate was also considered. However, efforts to locate the transition structure for a fully dissociative process computationally inevitably led to transition structures for the concerted elimination pathway (Figure 4). Moreover, such a mechanism would predict identical deuterium kinetic isotope effects on both the rearrangement and the elimination processes, which are not observed experimentally (Table 2). Finally, the >1% ^{13}C isotope effect seen at C9 in the enzymatic reactions (Table 1) also argues against a stepwise mechanism, because the bond order to C9 is not expected to decrease substantially in such a process. Although the C–C–O–C torsional mode would be lost in the enolate intermediate, this will not give a full 1% isotope effect.
(30) Guilford, W. J.; Copley, S. D.; Knowles, J. R. *J. Am. Chem. Soc.* **1987**, *109*, 5013–5019.
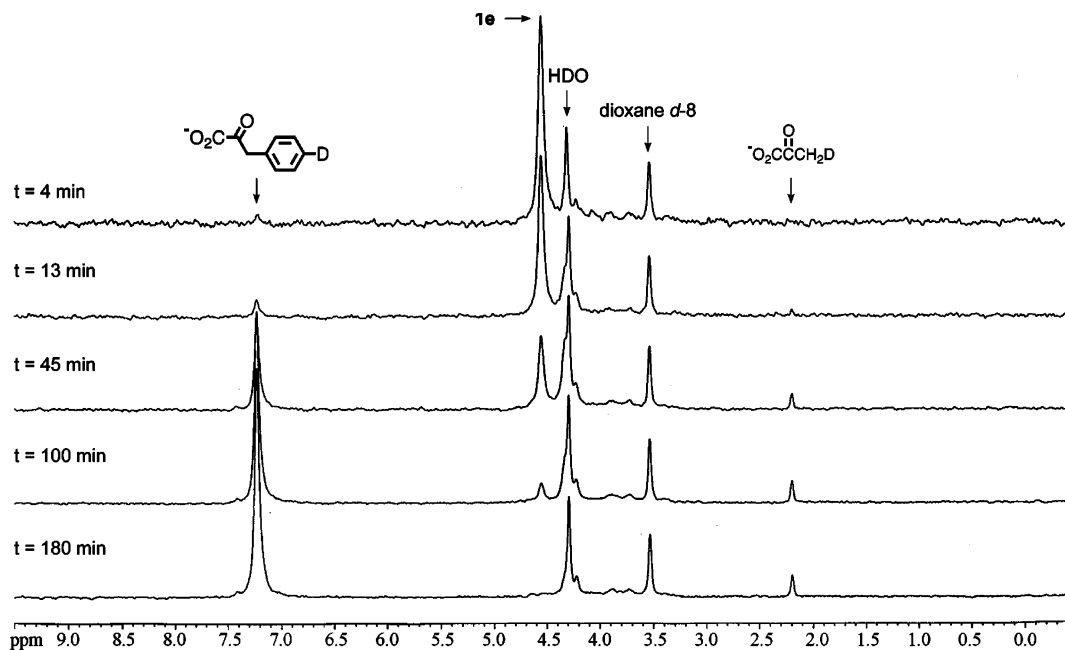
Figure 2. Decomposition of [4-^{2}H]chorismate (**1e**) in 100 mM phosphate buffer at pH 6.0 and 60 °C monitored by ^{2}H NMR spectroscopy.
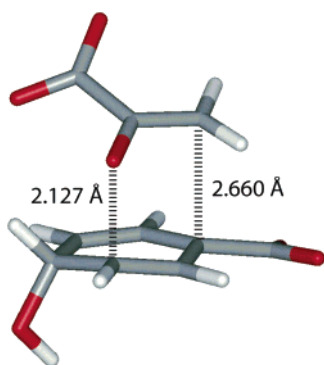
Figure 3. Becke3LYP/6-31+G* transition structure for the Claisen rearrangement of chorismate.

revert to chorismate.[29] The significant isotope effects observed at both C1 and C9, the two ends of the reacting π system, strengthen the conclusion that the C−C bond is partially formed in the transition state.

Significant slowing of the BsCM-catalyzed reaction by viscosogens such as glycerol points to the chemical step being only partially rate determining in this system.[13] As a consequence, the intrinsic isotope effects may not be fully expressed. Consistent with this possibility, the sluggish C75S variant, which is insensitive to changes in microviscosity,[13] exhibits a significantly larger ^{18}O isotope effect than BsCM itself or the theoretical prediction.[9] Moreover, the ^{13}C isotope effects at C1 and C9 are somewhat smaller than predicted by theory (Table 1). Together, these data imply that the enzymatic reaction may have a more dissociative transition state than the thermal process. Such a species could be stabilized by ionic groups that line the active site,[7] including Arg90, which directly contributes a hydrogen bond to the ether oxygen of chorismate in the transition state.[31] Hartree−Fock calculations support the ability of such interactions to alter the reactant and transition state

electronically relative to their gas-phase counterparts,[3a,32] although the computed C5−O7 and C1−C9 distances for the enzyme-bound transition state are longer and shorter, respectively, than found experimentally. These discrepancies probably reflect a combination of experimental inaccuracy, chemical differences between the wild-type and mutant enzymes, and computational limitations with such large systems.

EcCM, the second enzyme examined in this study, is representative of the AroQ family of chorismate mutases. It is evolutionarily unrelated to BsCM, but exhibits similar steady-state parameters[14,33] and has a comparably configured active site.[6] In this case, the isotope effects closely match the predicted values (Tables 1), indicating that an ionic active site environment need not necessarily alter the structure of the Claisen transition state. However, this conclusion rests on the uncertain assumption that chemistry is fully rate determining in this system. Although viscosogens have no effect on EcCM activity,[13] it is conceivable that a kinetically significant, but isotopically insensitive, conformational isomerization of bound chorismate precedes the actual rearrangement. This step might correspond to conversion of chorismate from its preferred pseudoequatorial conformation to a pseudoaxial conformation in which the carboxyvinyloxy group is aligned for reaction.[34] Such a scenario has been proposed to explain why isotope effects on the reaction catalyzed by the related *E. coli* chorismate mutase-prephenate dehydrogenase are suppressed.[1]

In the absence of enzyme, conversion of chorismate to 4-hydroxybenzoate and pyruvate competes with the Claisen rearrangement leading to prephenate.[4] As in the transformation of 3-(methoxycarbonyl)-5-ethenoxycyclohexadiene-*cis*-6-*d* to give methyl benzoate and CH$_2$DCHO,[26] this side reaction occurs via a concerted pericyclic mechanism in which C9 removes a proton (deuteron) from C4 rather than adding to C1 (Scheme

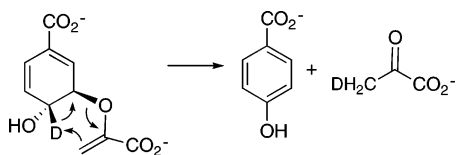(31) Kienhöfer, A.; Kast, P.; Hilvert, D. *J. Am. Chem. Soc.* **2003**, *125*, 3206−3207.

(32) Worthington, S. E.; Roitberg, A. E.; Krauss, M. *Int. J. Quantum Chem.* **2003**, *94*, 287−292.

(33) Stewart, J.; Wilson, D. B.; Ganem, B. *J. Am. Chem. Soc.* **1990**, *112*, 4582−4584.

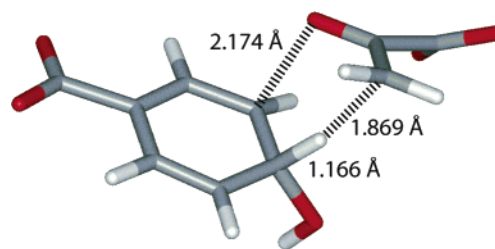(34) Copley, S. D.; Knowles, J. R. *J. Am. Chem. Soc.* **1987**, *109*, 5008−5013.

Scheme 5

5). Substantial transfer of deuterium from C4 of chorismate to pyruvate is observed, arguing against the involvement of an external base. The amount of label lost to solvent (ca. 40% after 3 h reaction) is readily explained by exchange under the experimental conditions. The ^2H isotope effect on the elimination (1.85 ± 0.06) is similar in magnitude to that observed for 3-(methoxycarbonyl)-5-ethenoxycyclohexadiene-*cis*-6-*d*. In addition, like the Claisen rearrangement, elimination of the enolpyruvyl group is subject to a large ^{18}O isotope effect at O7 (1.0374 ± 0.0005). These results show that the C—O bond is substantially cleaved in the transition state but that transfer of the hydrogen from C4 to C9 is not far advanced, in qualitative agreement with theoretical calculations (Figure 4, Table 2).[23] Both reactions, elimination and rearrangement, thus appear to be concerted but highly asynchronous.

Although the elimination is a minor side reaction thermally, the enzyme chorismate pyruvate-lyase efficiently converts chorismate to 4-hydroxybenzoate for the ubiquinone biosynthetic pathway.[35] Our results suggest that the latter enzyme and the related isochorismate pyruvate-lyase, which converts isochorismate to salicylate for the biosynthesis of many siderophores,[36] might operate by otherwise rare pericyclic mechanisms.

In summary, competitive experiments with isotopically labeled chorismate derivatives have provided direct information

(35) Siebert, M.; Severin, K.; Heide, L. *Microbiology-UK* **1994**, *140*, 897–904. Holden, M. J.; Mayhew, M. P.; Gallagher, D. T.; Vilker, V. L. *Biochim. Biophys. Acta-Protein Struct. Mol. Enzymol.* **2002**, *1594*, 160–167.
(36) Serino, L.; Reimmann, C.; Baur, H.; Beyeler, M.; Visca, P.; Haas, D. *Mol. Gen. Genet.* **1995**, *249*, 217–228. Serino, L.; Reimmann, C.; Visca, P.; Beyeler, M.; Della Chiesa, V.; Haas, D. *J. Bacteriol.* **1997**, *179*, 248–257. Gaille, C.; Kast, P.; Haas, D. *J. Biol. Chem.* **2002**, *277*, 21768–21775.

Figure 4. Becke3LYP/6-31+G* transition structure for the conversion of chorismate to 4-hydroxybenzoate.

about the nature of the transition state of the chorismate mutase reaction both in solution and at the active sites of evolutionarily unrelated enzymes. In all cases, the reaction proceeds via a pericyclic transition state in which C—C bond formation lags considerably behind C—O bond cleavage. Excellent quantitative agreement between theory and experiment is found for the uncatalyzed reaction, whereas the ionic active site of the enzymes may polarize the transition state somewhat as compared to its solution counterpart. The competing reaction of chorismate leading to 4-hydroxybenzoate, an intermediate in ubiquinone biosynthesis, likewise appears to occur via an asynchronous concerted mechanism. The latter finding raises the intriguing possibility that additional protein catalysts promoting pericyclic processes will be found.

Supporting Information Available: Coordinates and computational details for calculation of the theoretical isotope effects, plus derivations of eqs 2 and 3. This material is available free of charge via the Internet at http://pubs.acs.org.

JA052929V